A distributed-feedback fibre laser based optical fibre hydrophone system with very high-sensitivity

Author:
Peng, Gang-Ding; Leung, Ian; Brodzeli, Zourab; Whitbread, Trevor; Chen, Xiao-Bao

A distributed-feedback fibre laser based optical fibre hydrophone system with very high-sensitivity

Ian Leung[1], Zourab Brodzeli[1], Trevor Whitbread[1], Xiao-Bao Chen[2], Gang-Ding Peng[1]

[1] Photonics and Optical Communications Group
School of Electrical Engineering and Telecommunications
The University of New South Wales
Sydney 2052, Australia
Phone: +61-2-9385 5411 Fax: +61-2-9385 5993 Email: G.Peng@unsw.edu.au

[2] The Electronics 23rd Research Institute
China Electronic Technology Group Corporation
35 Yi Xian Road, Shanghai 200437

ABSTRACT

This paper reports the development of a very compact and very-high sensitivity optical fibre hydrophone system using a distributed-feedback fibre laser with a cavity length of 10cm. A theoretical system design making use of a Mach-Zehnder interferometer, homodyne demodulation scheme and digital signal processing is described. At the time of writing, the system is only partially completed; therefore the content of this paper will focus on the distributed-feedback fibre laser sensor head. Results for noise spectrum below 100kHz are presented, as well as discussions on some key issues with designing such hydrophone systems. Although not the intention for the system, initial results also indicate the suitability of the DFBFL for intensity modulated sensing.

Keywords: Distributed-feedback fibre laser, hydrophone, acoustic sensing, pump noise

1. INTRODUCTION

Optical fibre hydrophones have been developing over the past three decades, from the simple primary coated fibre immersed in water, to mandrel designs, to highly sensitive fibre laser based designs. Apart from being more sensitive than conventional ceramic hydrophones, optical fibre hydrophones also inherit the advantages of general fibre sensors, such as immunity to electromagnetic interference, down-lead insensitivity to disturbances, electrically passive, small size, light weight and relative simplicity in multiplexing designs. Fibre hydrophone systems have been developed mostly for military and geophysical applications. Strong interests exist for new photonic sensors replacing the conventional ceramic sensors, which can improve cost and reliability benefits for data acquisition operations.

In this paper we report the development of a very compact and very-high sensitivity optical fibre hydrophone system using distributed-feedback fibre laser (DFBFL). DFBFLs are single mode lasers with extremely narrow linewidths. A DFBFL with 10cm cavity length, made with modern fibre and grating writing techniques can act as a very compact sensing element, whose lasing wavelength is highly sensitive to acoustic pressure. We also show theoretically how an interrogation system consisting of a Mach-Zehnder interferometer (MZI), homodyne demodulation scheme using phase generated carrier and digital signal processing (DSP) could be implemented to detect the wavelength shifts.

2. THEORY

2.1   Distributed-feedback fibre laser (DFBFL)

A DFBFL consists of a pair of wavelength matched fibre Bragg gratings (FBG) written in a short section of Erbium doped fibre (EDF), shown in Figure 1. It is essentially a Fabry Perot structure, where the FBG separation is a quarter of one Bragg wavelength, producing a phase step within the length of the grating. When optically pumped with light of a shorter wavelength, the DFBFL will emit stimulated emission with a narrow bandwidth about the Bragg wavelength, such that the transmission peak appears in the center of the stop band. The specific wavelength and line width is determined by the transfer function of the gratings, the Fabry Perot response of the cavity, and gain narrowing due to the emission bandwidth of the EDF.
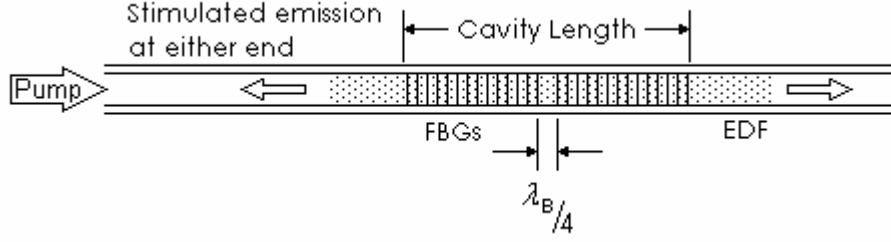
Figure 1. DFB fibre laser

In the presence of acoustic fields, strain $\Delta \varepsilon_{FL}$ will cause the DFBFL to undergo dimensional and refractive index changes, which leads to a change in the lasing wavelength $\Delta \lambda_{FL}$ (or change in lasing frequency $\Delta \nu_{FL}$). Similar response can be anticipated from a Distributed Bragg Reflector Fibre Laser (DBRFL)[4].

For FBG, the change in the Bragg wavelength $\Delta \lambda_B$ due to ambient pressure can be calculated using

$$\Delta \lambda_B = 2 n_e \Lambda \varepsilon_z - 2 n_e \Lambda \left(\frac{n_e^2}{2} ((\rho_{11} + \rho_{12}) \varepsilon_r + \rho_{12} \varepsilon_z) \right) \tag{1}$$

Where n_e is the effective refractive index. $\Lambda = \dfrac{\lambda_B}{2 n_e}$ is the grating pitch of the FBGs. ε_z and ε_r are the in-fibre pressure induced longitudinal and radial strains. Under hydrostatic boundary conditions, $\varepsilon_z = \varepsilon_r$. ρ_{11}, ρ_{12} are the elasto-optic coefficients, also known as the Pockel's (piezo) coefficients of the stress-optic tensor. The first term $2 n_e \Lambda \varepsilon_z$ corresponds to the physical length change, and the second term for change in refractive index. The two terms are usually in opposition, but the first term is dominant by a factor of 2.

Since the DFBFL emission is centered at the Bragg wavelength, ie. $\lambda_B = \lambda_{FL}$, (1) can be applied to calculate the DFBFL wavelength shift

$$\frac{\Delta \lambda_{FL}}{\lambda_{FL}} = \left(\varepsilon_z - \frac{n_e^2}{2} ((\rho_{11} + \rho_{12}) \varepsilon_r + \rho_{12} \varepsilon_z) \right) \tag{2}$$

Thus a change in the ambient pressure ΔP causing $\Delta \varepsilon_{FL}$ will lead to a change in DFBFL wavelength $\Delta \lambda_{FL}$.

2.2 Mach-Zehnder interferometer (MZI)

A MZI can be used to improve the resolution of the wavelength change $\Delta\lambda_{FL}$ of a single mode source. The phase output ϕ_{MZI} of a MZI is dependent on the wavelength of the DFBFL

$$\phi_{MZI} = \frac{2\pi n_e L_{MZI}}{c} \nu_{FL} = \frac{2\pi n_e L_{MZI}}{\lambda_{FL}} \qquad (3)$$

where L_{MZI} is the physical path difference between the two fibre arms, and so

$$\frac{\partial \phi_{MZI}}{\partial \lambda_{FL}} = \frac{-2\pi n_e L_{MZI}}{\lambda_{FL}^2} \qquad (4)$$

(4) shows that the phase shift change per unit wavelength change is directly proportional to the optical path difference. In other words, inserting a longer path difference will produce larger phase shift per unit strain at the MZI output of the hydrophone system. This allows the use of a short section of fibre laser to replace a much longer section of sensing fibre required for mandrel designs, greatly reducing the size of the sensor head. The maximum optical path difference is limited by the coherence length of the DFBFL

2.3 Linewidth measurement

The coherence length of the DFBFL can be determined by measuring the linewidth. Delayed self-heterodyne and delayed self-homodyne are linewidth measurement techniques which could be performed also with a MZI. These techniques require the delay time between the two arms exceed the coherence time of the source, so that the two combining beams appear to be from two independent sources. The latter technique is the less complicated of the two, and produces a beat tone at 0Hz that is broadened by the laser linewidth.

2.4 Homodyne demodulation using phase generated carrier

A homodyne detection scheme using phase generated carrier can detect phase shifts in the microradian range[6]. Sinusoidal modulation with frequency ω_0 and amplitude C can be applied to one arm of the MZI by means of a piezo-electric stretcher. Then the variation in the light intensity detected at the output can be described as

$$I = A + B\cos(C\cos\omega_0 t + \phi(t)) \qquad (5)$$

where A and B are proportional to the optical power of the two arms, but B also depends on the mixing efficiency. The phase signal $\phi(t)$ can be obtained by mixing the output with proper multiples of ω_0 and low-pass filtering to remove higher order terms. The procedure is depicted in Figure 2 for up to the $2\omega_0$ component, where G and H are the amplitude of the mixing signals.

To obtain $\phi(t)$, two signals, one containing $\sin\phi(t)$, the other containing $\cos\phi(t)$ are required. $\phi(t)$ can be recovered by integrating the difference between the cross multiplied time derivatives of the $\sin\phi(t)$ and $\cos\phi(t)$ signals.

2.5 Digital signal processing (DSP)

The hydrophone system becomes much more robust by converting the optical detector output into digital data. Doing so also makes possible the application of powerful DSP techniques for filtering and noise reduction. However, the maximum frequency of interest must be less than half the sampling frequency. Therefore, a low pass filter should be implemented between the detector and the data acquisition card (DAQ) to prevent aliasing and frequency folding.
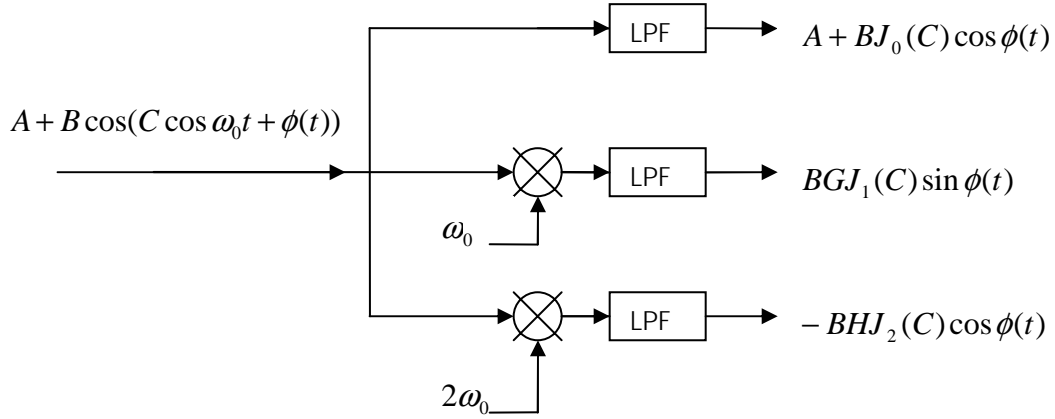
Figure 2. Procedure to obtain sine and cosine of phase shift $\phi(t)$.

3   EXPERIMENT SETUP

The system setup is depicted in Figure 3. The DFBFL has a cavity length of 10cm. It is single polarization, with RIN < 80dB/Hz, and center wavelength at 1551.2nm. A SDL 980nm laser diode was used to remotely pump the DFBFL through the down-lead fibre. The SDL laser diode is powered using a Newport 505 Laser Diode Driver, and a Melles Griot 06 DTC 101 Thermoelectric Cooler Controller. A wavelength division (de)multiplexer (WDM) is used to channel the returning 1550nm region emission to (and direct any of the reflected 980nm away from) the rest of the system. An isolator is used to prevent scattering noise from returning and affecting the DFBFL emission spectrum.

For the results presented, the detector used was an Optiphase V500 Analog Receiver, which also have gain, high-pass and low-pass features. It is planned for the analog receiver to be replaced with a Fujitsu FID3S2kX Series Analog PIN Photodiode with extra electrical circuitry to realize gain and filtering functions. The analog output of the detector is then sampled using a NI PCI-6013. This DAQ has 16bit input resolution, maximum sampling rate 200kS/s, and input range of ±0.05 to ±10V. Low pass feature of the detector is adjusted according to the sampling rate, ie. Low-pass set to 100kHz for maximum sampling rate.
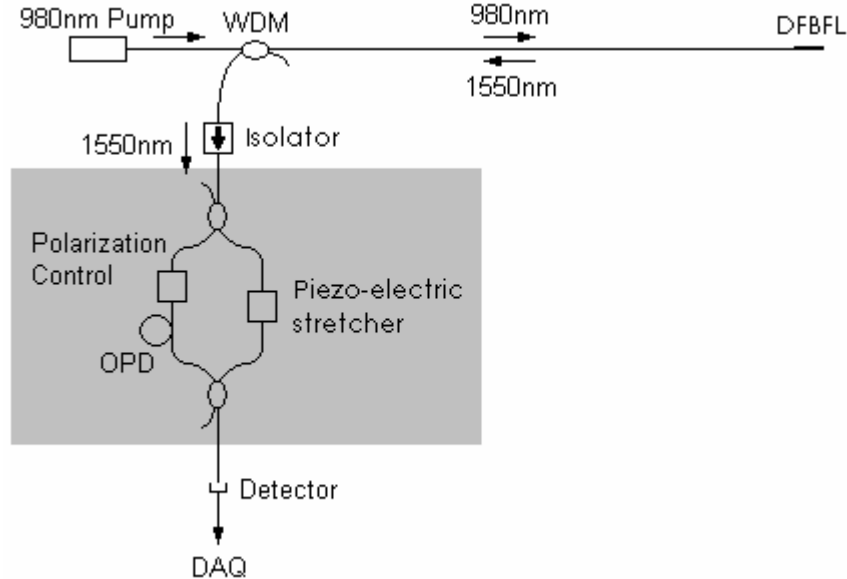

Figure 3. Experiment system.

The NI PCI-6013 is controlled with a LabView 7 Express program. The program also converts the time domain information into the frequency domain. Common windows such as Hanning, Hamming, Blackman and Harris can be applied to improve the signal to noise ratio (SNR) of the calculated frequency power spectrum. Various averaging operations can also be performed on the final spectrum.

At the time of writing this paper, isolation and power balancing problems associated with the MZI have not been completely resolved (indicated by the shaded area). Also, the phase generated carrier demodulation scheme has yet to be implemented. An Agilent 11896A Polarisation Controller is connected in series with the path difference fibre to form one arm of the MZI. It is planned for the demodulation scheme to be realised using a signal generator, a second sampling channel on the DAQ, and using DSP to perform the required differentiation, integration, low-pass filtering and other arithmetic operations. Alternatively, the signal generator can be omitted by using a DAQ which is capable of producing the desired frequency to drive the piezo-electric stretcher.

4   RESULTS
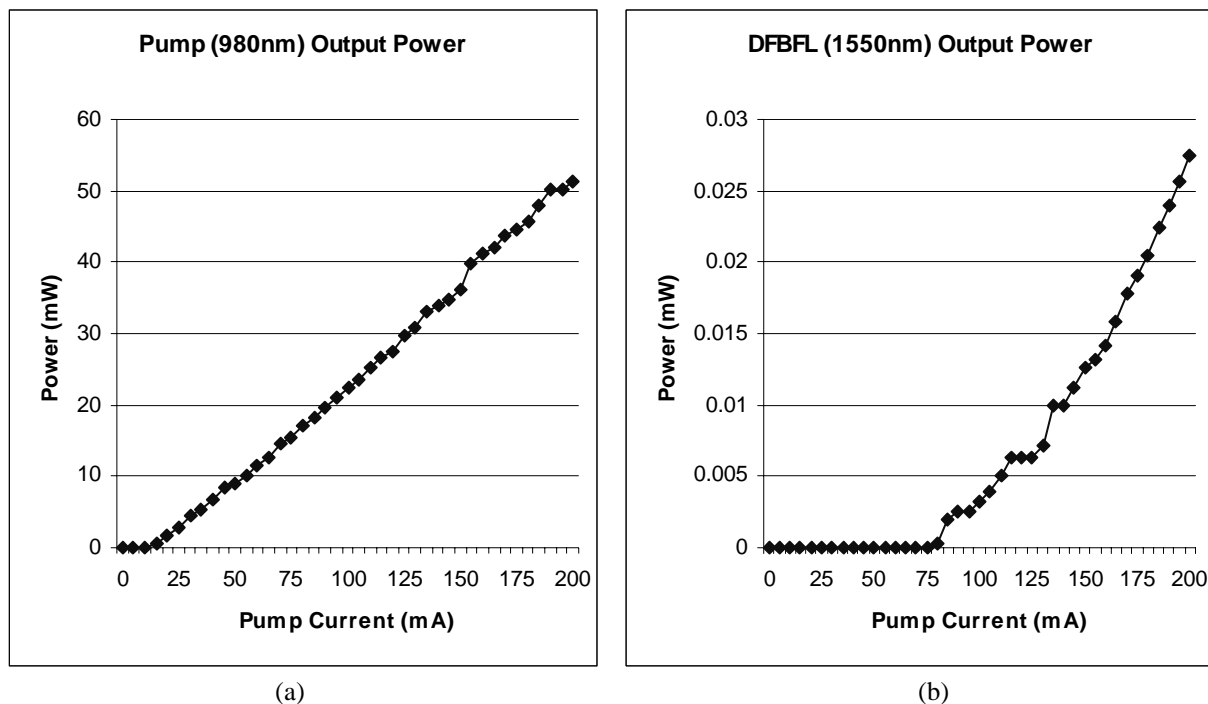
4.1   Threshold current

Figure 4. (a) Pump output power, (b) DFBFL output power, as a function of pump current.

The 980nm laser diode's driving current was controlled with a Newport 505 Laser Diode Driver, and an Agilent 86140B Optical Spectrum Analyser was used to measure the returning 1550nm power immediately after the WDM. It was noted that the condition of the down-lead fibre does affect the effective threshold current of this multi-stage process, by up to 50mA. The results show that the lowest effective threshold current is approximately 80mA, with efficiency of 0.2μW/mA beyond threshold. (Figure 4)

4.2   Bragg gratings mismatch

It was found that the Bragg wavelengths of the pair of FBGs of the DFBFL were not ideally matched. Warming one end of the cavity through simple means of placing hand adjacent (without touching) to it will cause the amplitude of the sampled time signal to drop noticeably. Warming the other end causes the amplitude to increase instead. Although this is undesirable for the intent of this system, it demonstrated the possibility of using a DFBFL for temperature sensing applications.

4.3   Initial sensing test

To test the DFBFL's suitability for hydrophone applications, and the compatibility of the so-far-completed portion of the system, a speaker was placed next to the sensor head. A 1.5kHz sinusoidal signal from a signal generator was applied to the speakers. By varying the amplitude of the 1.5kHz sinusoidal signal, a corresponding change in the power of 1.5kHz component of the calculated spectrum was observed. This result demonstrated the suitability of the DFBFL for intensity sensing.

It should first be mentioned that for all frequency spectrums shown in this paper, the displayed unit of the spectrum strength is dB. It was verified that the sharp 60dB contrast in spectrum strength was indeed caused only by the calculated 0Hz value. Vast improvement of the SNR was observed by applying DSP averaging operations on the calculated spectrum. In figure 5(a), The amplitude of the 1.5kHz signal was reduced until it was just visible on the calculated spectrum. Results under the same conditions, with exponentially-weighted RMS averaging (50 averages) applied is shown in Figure 5(b). These results, although obtained under a much lower pump power (~40mW), share a similar profile to the results demonstrated by Hill and co-workers[4] (110mW pump power).
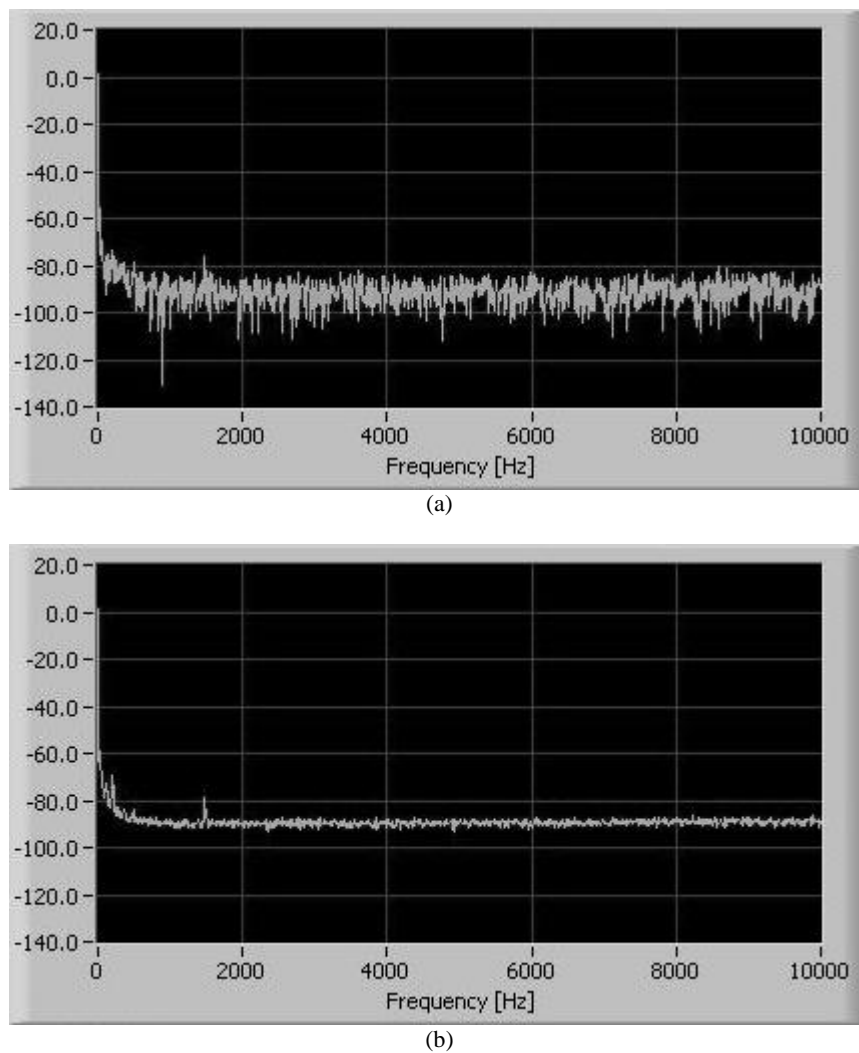

(a)

(b)

Figure 5. 200kHz sampling frequency, 40k samples, 160mA pump current. (a) no averaging, (b) exponentially-weighted RMS averaging (50 averages).

4.4 Isolator

Without applying any averaging, the spectrum with and without the isolator inserted was compared. It was observed that the DC level of the sampled time signal was reduced from 1.4V to 0.9V if an isolator was inserted. However, as shown in Figure 6, the noise spectrum below 2kHz was suppressed by 20dB.
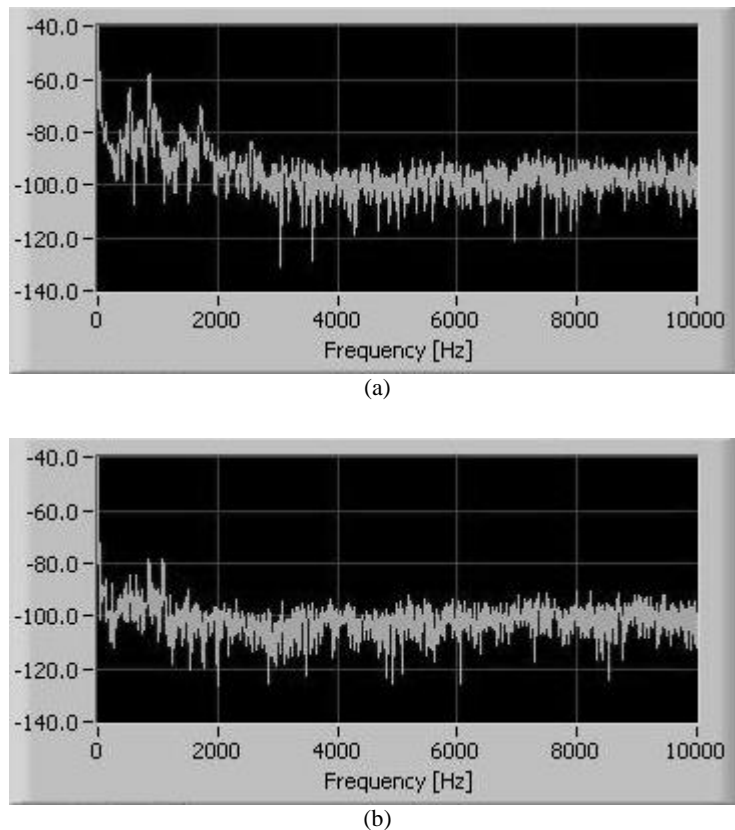

(a)

(b)

Figure 6. 200kHz sampling frequency, 40k samples, 160mA pump current, no averaging. (a) no isolator (b) with isolator.

4.5 Pump noise spectrum

As mentioned in section 4.1, the effective threshold current can be varied by disturbing the down-lead fibre. From the DFBFL standpoint, such disturbances is similar to varying the received 980nm power, or pump current. Therefore, the dynamics between low pump currents and the calculated spectrum is of interest. Figure 7 displays 2 sets of representative spectrums, under different pump drive currents.

When the DFBFL is just above threshold (90mA pump current, ~20mW pump output), a distinct fundamental peak at 30kHz and its harmonics can be observed (Figure 7(c), (d)) The profile of the peaks was verified not to be aliases by repeating using different sampling frequencies. As the pump current is increased, these frequency peaks also increase. At 150mA pump current, the fundamental peak was moved to 90kHz. The small peak that appears to be at 20kHz is actually an alias caused by the folding of the first harmonic at 180kHz due to the sampling process (Figure 7(e)). This was verified by reducing the low pass frequency to 33kHz on the receiver, causing the peak at 20kHz to disappear. Depending on the frequency response of interest of the hydrophone (typically < 20kHz), power levels which causes the noise peaks to appear in the band of interest should be avoided, in order to minimize the noise floor.

The position of the fundamental peaks with respect to pump current is plotted in Figure 8. The results show that, beyond threshold, the position of the fundamental frequency peak seem to increases linearly with pump current (and power). It was speculated that the peaks are caused by imperfections in the DFBFL, or by the pumping process.
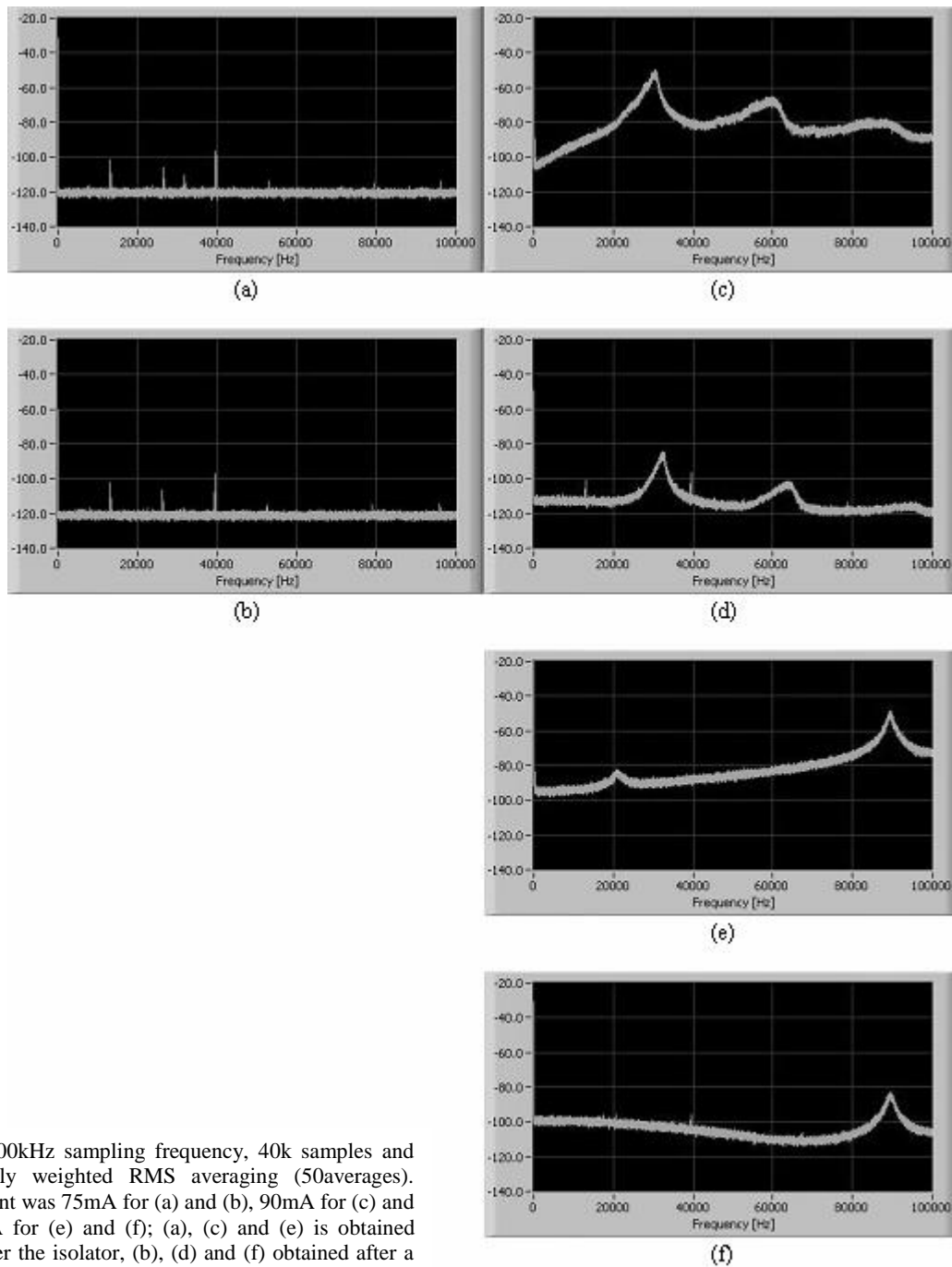
Figure 7. 200kHz sampling frequency, 40k samples and exponentially weighted RMS averaging (50averages). Pump current was 75mA for (a) and (b), 90mA for (c) and (d), 150mA for (e) and (f); (a), (c) and (e) is obtained directly after the isolator, (b), (d) and (f) obtained after a MZI with 50km path difference.

As can be expected, longer fibre lengths reduces the signal strength, and hence the spectrum strength is also reduced. It was noted that for a 50km path difference MZI, the amplitude of the sampled time signal was less than 0.1V, suggesting that power equalization is an issue which needs to be addressed. However, the frequency peak features can still be clearly identified, once again demonstrating the benefits of digitizing the signal.
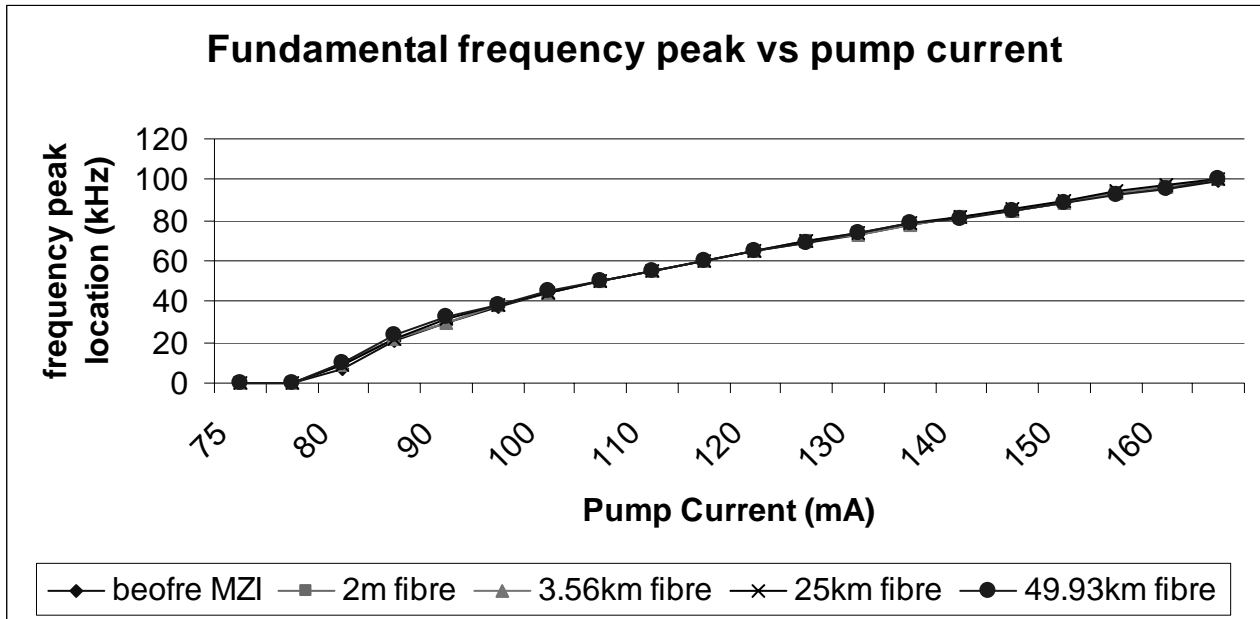
Figure 8. Position of fundamental frequency peak as function of pump current.

4.6 Linewidth measurement

As outlined in section 2.2, the linewidth of the DFBFL needs to be measured, so that the appropriate path difference can be determined to optimize the performance of the MZI. Since the problems of isolation of the ultra-high sensitivity DFBFL sensor head, and isolation of the MZI are not yet fully resolved, only rough and preliminary results are presented for linewidth measurement. Again, power equalization needs to be considered to ensure better mixing efficiency.

It was assumed that the condition of delay time exceeding the coherence time of the DFBFL was satisfied by using a 25km path difference. Preliminary results indicates the 3dB linewidth to be between 10kHz to 20kHz. (Figure 9)
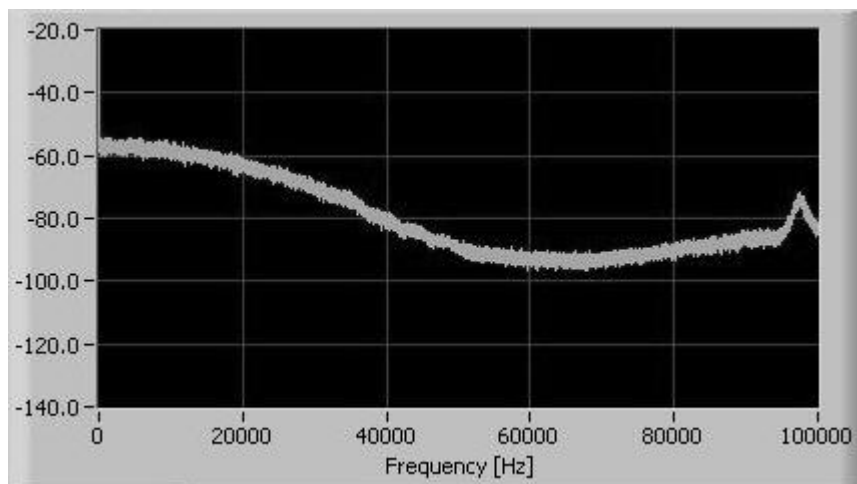

Figure 9. 200kHz sampling frequency, 40k samples, 160mA pump current, exponentially weighted RMS averaging (50averages), and using MZI with 25km path difference.

5   CONCLUSION & DISCUSSION

It was shown how a very-high sensitivity hydrophone system employing a distributed-feedback fibre laser can be theoretically implemented. Although not the intention of the hydrophone system, undesirable characteristics and the initial results demonstrated the opportunities of using a distributed-feedback fibre laser for intensity modulated (lower resolution) sensing applications. Digitizing the data allows the application of Fourier transform, resulting in clear spectral description even at low signal amplitudes. To improve sensitivity, proper isolation of the MZI is essential. Power equalisation between the two arms of the MZI are also necessary to ensure good optical mixing efficiency. Also, high-quality isolation of the sensor head is required to obtain accurate linewidth measurements, so that the resolution of the system can be optimized. The presence of pump noise within the hydrophone's operational frequency band can be avoided by using higher pump currents. Other sensitivity improvement techniques such as applying coating materials should also be considered.

6   REFERENCES

1.   A. Dandridge and G.B. Cogdell, *'Fiber Optic Sensors for Navy Applications'*, IEEELCS, pp.81-89, Feb. 1991
2.   A.D. Kersey and A. Dandridge, *'Applications of Fiber-Optic Sensors'*, IEEE Transactions on Components, Hybrids, and Manufacturing Technology, Vol. 13, No. 1, pp.137-143, Mar. 1990
3.   A.D. Kersey, M.A. Davis, H.J. Patrick, M. LeBlanc, K.P. Koo, C.G. Askins, M.A. Putnam and E.J. Friebele, *'Fiber Grating Sensors'*, IEEE J. Lightwave Tech., Vol. 15, No. 8, pp.1442-1463, Aug. 1997
4.   D.J. Hill, P.J. Nash, D.A. Jackson, D.J. Webb, S.F. O'Neill, I. Bennion and L. Zhang, *'A fiber laser hydrophone array'*, SPIE Vol. 3860, pp.55-66, Sep. 1999
5.   K.P. Koo and A.D. Kersey, *'Bragg Grating-Based Laser Sensors Systems with Interferometric Interrogation and Wavelength Division Multiplexing'*, IEEE J. Lightwave Tech., Vol. 13, No. 7, pp.1243-1249, Jul. 1995
6.   A. Dandridge, A.B. Tveten and T.G. Giallorenzi, *'Homodyne Demodulation Scheme for Fiber Optic Sensors Using Phase Generated Carrier'*, IEEE Transactions on Microwave Theory and Tech., Vol. MTT-30, No. 10, pp.1635-1641, Oct. 1982